J. Fluid Mech. (1968), *vol.* 33, *part* 2, *pp.* 209–225
Printed in Great Britain

Maximum dissipation resulting from lift in a slow viscous shear flow

By E. Y. HARPER† AND I-DEE CHANG

Department of Aeronautics and Astronautics, Stanford University, Stanford, California

(Received 11 May 1967 and in revised form 9 January 1968)

The lift tensor for any three-dimensional body moving in a linear shear flow at low Reynolds numbers has been calculated by asympototic methods. The tensor is applied to the problem of the motion of a dumb-bell shaped particle. The particle is shown to have a preferred periodic orbit which corresponds to maximum dissipation. The dissipation is calculated and the intrinsic viscosity of a dilute suspension of such particles is predicted. Experiments conducted with a single particle tend to confirm the stability of the predicted orientation.

1. Introduction

The so-called intrinsic viscosity, ν, of a dilute suspension of particles in a homogeneous fluid of viscosity μ_0 is defined by

$$\mu = \mu_0(1 + \nu c), \tag{1}$$

where μ is the viscosity of the suspension and c is the volume concentration of the particles. Einstein (1905) and Brenner (1958) have shown that the intrinsic viscosity for a dilute suspension of spheres is $\frac{5}{2}$. Jeffery (1922) calculated the intrinsic viscosity for ellipsoidal particles in a linear shear flow using Stokes's equations. However, his solution was indeterminate in the sense that the motion, which is periodic, depends upon the initial conditions of release of the particle. In order to obtain more definite results Jeffery hypothesized that 'the particle will tend to adopt that motion which, of all the motions possible under the approximated equations, corresponds to the least dissipation of energy'. Taylor (1923) reported experimental results which appeared to verify Jeffery's minimum dissipation hypothesis, at least for the case of spheroids. Saffman (1956) indicated that the effect of fluid inertia on spheroidal particles is to alter slowly the orbit of the particle in a direction consistent with Jeffery's hypothesis. However, the magnitude of the predicted inertia effect was too small to account for Taylor's experiments.

Christopherson & Dowson (1959) analysed the motion of a sphere moving slowly down a tube whose inner diameter was only slightly in excess of the sphere diameter. A particular eccentricity of the sphere was found to correspond to minimum dissipation, and experiments were conducted to see whether the sphere would assume this eccentricity. Exact verification was not possible and

† Now at Lockhead Palo Alto Research Laboratory.

the authors concluded that 'all that can be asserted at this stage is that for very small velocities of descent the minimum dissipation criterion has been approximately vertified'. The authors go on to say, 'so far as is known, this particular system of a ball in a close-fitting tube has no practical application. It might therefore be rewarding to seek other systems in which the minimum hypothesis can conveniently be tested rather than endeavouring to refine the methods by which observations on this one can be made.'

At this point it should be mentioned that cases of maximum dissipation have been reported. Cox (1965) has demonstrated analytically that the second-order effect of fluid inertia is to orient settling disks and rods so that their resistance is a maximum. Mason, Karnes & Goldsmith (1963) conducted experiments in which disks and rods assumed maximum dissipative orbits when undergoing Couette flow at moderate Reynolds numbers.

One purpose of the present paper is to demonstrate, analytically, that, even within the restricted class of flows considered by Jeffery, the minimum dissipation hypothesis does not hold. We will consider the effect of fluid inertia on a bouyantly neutral dumb-bell shaped particle in a linear shear flow. The motion of the particle will be determined by employing a lift tensor, derived in appendix A for any three-dimensional body, to the case of a sphere. The lift tensor will be obtained by generalizing the original result of Saffman (1965), who found that the sphere experiences a component of lift due to fluid inertia which, to the order given, is independent of the spin (for reasonable spin rates). It is this inertial lift which renders the dumb-bell motion aperiodic and moves it to its final preferred orientation.

2. Analysis

Consider a dumb-bell shaped body (figure 1), composed of two neutrally bouyant spheres of radius a, constrained to remain with centres a distance $2l$ apart. The parameter $\epsilon = a/l$ is considered to be a fixed number, small compared with unity. We define two cartesian co-ordinate systems whose origins remain coincidental at the point of symmetry half-way between the spheres. The first, or unprimed, co-ordinate system is fixed in the body with the x-axis connecting the centres of the two spheres. The unit vectors $\mathbf{i}$, $\mathbf{j}$, $\mathbf{k}$ are associated with the x, y, z axes. The second, or primed, co-ordinates are fixed in space and have unit vectors $\mathbf{i}'$, $\mathbf{j}'$, $\mathbf{k}'$ associated with the $\mathbf{x}'$, $\mathbf{y}'$, $\mathbf{z}'$ axes. The undisturbed flow field, $\mathbf{V}$, is considered to be a linear shear flow,

$$\mathbf{V} = \kappa y' \mathbf{k}. \tag{2}$$

The direction cosines between the two co-ordinate systems are given by

$$\left.\begin{aligned} \mathbf{i}' &= l_1\mathbf{i} + l_2\mathbf{j} + l_3\mathbf{k}, \\ \mathbf{j}' &= m_1\mathbf{i} + m_2\mathbf{j} + m_3\mathbf{k}, \\ \mathbf{k}' &= n_1\mathbf{i} + n_2\mathbf{j} + n_3\mathbf{k}. \end{aligned}\right\} \tag{3}$$

The co-ordinate systems and direction cosine notation have been chosen in order to facilitate comparison with Jeffery's analysis for an ellipsoid. Distinguishing the two spheres as A and B, we define the difference between the velocity of

sphere A, and the undisturbed velocity $\mathbf{V}^A$ at the centre of A, as $\mathbf{U}^A$. The force on sphere A is denoted by $\mathbf{F}^A$ while the torque on the dumb-bell due to sphere A is $\mathbf{T}^A$. Neglecting the interaction between spheres A and B we have

$$\mathbf{T}^A = l\mathbf{i} \times \mathbf{F}^A + \mathbf{T}_S^A, \tag{4}$$

where $\mathbf{T}_S^A$ is the torque arising from the rotation of sphere A and the vorticity of the fluid,

$$\frac{\mathbf{T}_S^A}{4\pi\mu_0 a^3} = [(\nabla \times \mathbf{V})_A - \omega_x \mathbf{i}] = [\kappa \mathbf{i}' - \omega_x \mathbf{i}]. \tag{5}$$

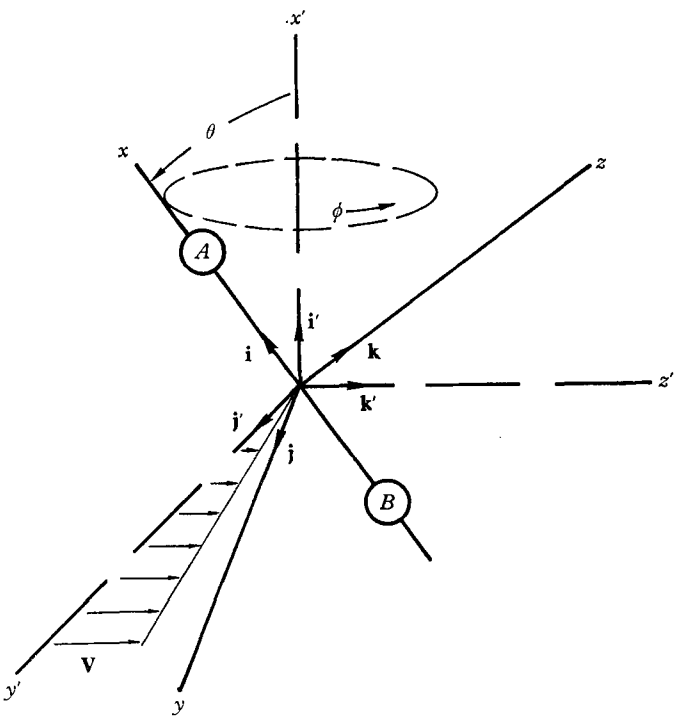

FIGURE 1. Co-ordinate systems for the dumb-bell shaped particle.

We then have

$$\mathbf{T}^A = 4\pi\mu_0 a^3[\kappa l_1 - 2\omega_x]\mathbf{i} + [4\pi\mu_0 a^3 l_2 - lF_z]\mathbf{j} + [4\pi\mu_0 a^3 l_3 + lF_y]\mathbf{k}. \tag{6}$$

We may now evaluate F_y and F_z in terms of the Stokes drag and a higher-order force represented by a lift tensor $\mathscr{L}$,

$$F_i^A = 6\pi\mu_0 a U_i^A + \mathscr{L}_{ij} U_j^A, \tag{7}$$

and in turn express U_j^A in terms of $\boldsymbol{\omega}$. In principle, the resulting expression for the torque can be used to solve the equations of motion for a rigid body. However, it is possible to express the effects of fluid inertia to an order which is lower than the order of the inertia of the body. This allows us to obtain the motion, to the order of the body inertia, by setting the torque equal to zero. Saffman has shown that the lift tensor may be computed to $O(R_\kappa^{\frac{1}{2}})$, where

$$R_\kappa = \kappa a^2/\nu, \tag{8}$$

under the restriction that

$$R_\kappa \ll 1, \quad R_v \ll R_\kappa^{\frac{1}{2}}, \tag{9}$$

where R_v is the conventional Reynolds number based on sphere radius and relative fluid velocity. If we define an upper limit on R_v as

$$R_{v\max} = \kappa la/\nu = R_\kappa/\epsilon \tag{10}$$

and impose the restriction that

$$R_\kappa \ll 1, \quad R_\kappa^{\frac{1}{2}} \ll \epsilon, \tag{11}$$

the force on the sphere will be $O(R_\kappa^{\frac{1}{2}})$ whereas the body inertia is $O(R_\kappa)$.

The lift tensor will be denoted in space-fixed co-ordinates as

$$\mathscr{L}_{i'j'} = \begin{pmatrix} \mathscr{B} & 0 & 0 \\ 0 & \mathscr{C} & \mathscr{S} \\ 0 & \mathscr{U} & \mathscr{A} \end{pmatrix}. \tag{12}$$

After some manipulation, the components of $\mathbf{F}^A$, in body-fixed co-ordinates, may be expressed as

$$\left.\begin{aligned} F_y^A = 6\pi\mu_0 a U_y^A &+ [\mathscr{B}l_1l_2 + \mathscr{C}m_1m_2 + \mathscr{A}n_1n_2 + \mathscr{U}m_1n_2 + \mathscr{S}m_2n_1]\,U_x^A \\ &+ [\mathscr{B}l_2l_3 + \mathscr{C}m_2m_3 + \mathscr{A}n_2n_3 + \mathscr{U}m_3n_2 + \mathscr{S}m_2n_3]\,U_z^A \\ &+ [\mathscr{B}l_2^2 + \mathscr{C}m_2^2 + \mathscr{A}n_2^2 + \mathscr{U}m_2n_2 + \mathscr{S}m_2n_2]\,U_y^A, \\ F_z^A = 6\pi\mu_0 a U_z^A &+ [\mathscr{B}l_1l_3 + \mathscr{C}m_1m_3 + \mathscr{A}n_1n_3 + \mathscr{U}m_1n_3 + \mathscr{S}m_3n_1]\,U_x^A \\ &+ [\mathscr{B}l_2l_3 + \mathscr{C}m_2m_3 + \mathscr{A}n_2n_3 + \mathscr{U}m_2n_3 + \mathscr{S}m_3n_2]\,U_y^A \\ &+ [\mathscr{B}l_3^2 + \mathscr{C}m_3^2 + \mathscr{A}n_3^2 + \mathscr{U}m_3n_3 + \mathscr{S}m_3n_3]\,U_z^A. \end{aligned}\right\} \tag{13}$$

We must now express $\mathbf{U}^A$ in terms of $\boldsymbol{\omega}$:

$$\begin{aligned} \mathbf{U}^A &= \mathbf{V}^A - \boldsymbol{\omega} \times l\mathbf{i} \\ &= [\kappa l m_1 n_1]\mathbf{i} + [\kappa l m_1 n_2 - l\omega_z]\mathbf{j} + [\kappa l m_1 n_3 - l\omega_y]\mathbf{k} \\ &= U_x^A\mathbf{i} + U_y^A\mathbf{j} + U_z^A\mathbf{k}. \end{aligned} \tag{14}$$

From the Stokes solution of the equations of motion we find that U_x is $O(1)$ while U_y and U_z are $O(\epsilon^2)$. The component of relative velocity is largest along the axis connecting the spheres because it is the constraint between the spheres that causes the slip. In order to simplify the equations of motion we will drop terms of order $O(\epsilon^2 R_\kappa^{\frac{1}{2}})$ when (13) and (14) are combined. As we have already mentioned, terms of order $O(R_\kappa)$ will also be dropped. If we introduce the dimensionless quantities

$$\boldsymbol{\omega}^* = \frac{\boldsymbol{\omega}}{\kappa}, \quad \mathbf{F}^* = \frac{\mathbf{F}}{\mu_0 \kappa l a}, \tag{15}$$

the equations of motion become:

$$2\omega_x^* = l_1, \quad F_z^* = 4\pi\epsilon^2 l_2, \quad F_y^* = -4\pi\epsilon^2 l_3. \tag{16}$$

Defining

$$\mathscr{L}_{i'j'}^* = \frac{1}{6\pi\mu_0 a}\mathscr{L}_{i'j'} \tag{17}$$

and combining equations (13), (14) and (16), we obtain

$$\left.\begin{aligned}\omega_x^* &= \tfrac{1}{2}l_1,\\ \omega_y^* &= \tfrac{2}{3}\epsilon^2 l_2 - m_1 n_3 - \mathscr{S}^* m_1 m_3 n_1^2 - \mathscr{U}^* m_1^2 n_1 n_3\\ &\quad - m_1 n_1(\mathscr{B}^* l_1 l_3 + \mathscr{C}^* m_1 m_3 + \mathscr{A}^* n_1 n_3),\\ \omega_z^* &= \tfrac{2}{3}\epsilon^2 l_3 + m_1 n_2 + \mathscr{S}^* m_1 m_2 n_1^2 + \mathscr{U}^* m_1^2 n_1 n_2\\ &\quad + m_1 n_1(\mathscr{B}^* l_1 l_2 + \mathscr{C}^* m_1 m_2 + \mathscr{A}^* n_1 n_2).\end{aligned}\right\} \tag{18}$$

At this point we introduce the Euler angles θ, ϕ and ψ, where θ is the angle between the x- and x'-axes, ϕ is the angle between the $(x'y')$- and (x', x)-planes, and ψ is the angle between the (x', x)- and (x, y)-planes. Thus we have,

$$\left.\begin{aligned}\omega_x^* &= \cos\theta,\\ \omega_y^* &= \frac{d\theta}{dt^*}\sin\psi - \frac{d\phi}{dt^*}\sin\theta\cos\psi,\\ \omega_z^* &= \frac{d\theta}{dt^*}\cos\psi + \frac{d\phi}{dt^*}\sin\theta\sin\psi,\end{aligned}\right\} \tag{19}$$

and

$$\begin{aligned} m_1 &= \sin\theta\cos\phi,\\ m_2 &= \cos\theta\cos\phi\cos\psi - \sin\phi\sin\psi,\\ m_3 &= -\sin\phi\cos\phi - \cos\theta\cos\phi\sin\psi,\\ n_1 &= \sin\theta\sin\phi,\\ n_2 &= \cos\phi\sin\psi + \cos\theta\sin\phi\cos\psi,\\ n_3 &= \cos\phi\cos\psi - \cos\theta\sin\phi\sin\psi,\\ l_1 &= \cos\theta,\\ l_2 &= -\sin\theta\cos\psi,\\ l_3 &= \sin\theta\sin\psi. \end{aligned}$$

It is possible to obtain an ordinary differential equation for the nutation angle as a function of the precession angle without dropping any of the terms in (18). We obtain

$$\frac{d\phi}{d\theta} = \frac{\begin{aligned}&\sin\phi\cos\phi\sin\theta\cos\theta\{1+\sin^2\theta[(\mathscr{S}^*+\mathscr{U}^*)\sin\phi\cos\phi\\ &\qquad +\mathscr{A}^*\sin^2\phi+\mathscr{C}^*\cos^2\phi-\mathscr{B}^*]\}\end{aligned}}{\begin{aligned}&\cos^2\phi+\tfrac{2}{3}\epsilon^2+\sin\phi\cos\phi\sin^2\theta\{(\mathscr{U}^*\cos^2\phi-\mathscr{S}^*\sin^2\phi)\\ &\qquad +(\mathscr{A}^*-\mathscr{C}^*)\sin\phi\cos\phi\}\end{aligned}}. \tag{20}$$

3. Results

The Stokes solution, $R_\kappa = \mathscr{L}_{i'j'} = 0$, of (20) is periodic with period T, and is dependent on the initial condition, θ_0, analogous to Jeffery's result,

$$\theta = \tan^{-1}\frac{[1+\alpha(\epsilon)]^{\frac{1}{2}}\tan\theta_0}{[\cos^2\phi+\alpha(\epsilon)]^{\frac{1}{2}}}, \tag{21}$$

$$T = \frac{2\pi}{\kappa[\alpha(\epsilon)+\alpha^2(\epsilon)]^{\frac{1}{2}}}, \tag{22}$$

where $\theta_0 = \theta(\phi = 0)$ and $\alpha(\epsilon) = \frac{2}{3}\epsilon^2$. The properties of (20) for non-zero values of R_κ have been generally established by numerical integration. If the off-diagonal perturbations $\mathscr{S}^*$ and $\mathscr{U}^*$ are set to zero, the remaining perturbations have the effect of changing the shape of the Stokes orbit, (21), for a given value of θ_0 between 0 and $\frac{1}{2}\pi$. However, the motion remains periodic. This is because the diagonal perturbations act in the instantaneous direction of the sphere motion and the resulting torque is normal to the instantaneous plane of motion of the dumb-bell. The off-diagonal perturbations render the motion aperiodic, with the $\mathscr{S}^*$ perturbation exerting a much stronger influence than the $\mathscr{U}^*$ perturbation. This results from the fact that the $\mathscr{S}^*$ perturbation acts in the z'-direction as a result of relative velocity in the x'-direction, while the $\mathscr{U}^*$ perturbation acts in the x'-direction and is due to relative velocity in the z'-direction. The latter velocity changes sign in each quadrant, which tends to have a compensating effect, while the former slip is always in the same direction with respect to an observer on the particle. Therefore, if all the perturbation quantities are assumed to be of the same magnitude, the $\mathscr{S}^*$ perturbation determines the stability of the particle orbit, and it is not necessary to know the explicit values of the other perturbation quantities. The $\mathscr{S}^*$ perturbation has been found to be a positive quantity which causes the axis of the dumb-bell to move asympototically into the plane of the fluid motion; during this process the nutation angle never exceeds a value of $\frac{1}{2}\pi$. A position of unstable equilibrium exists when the dumb-bell axis coincides with the vorticity vector and the spheres rotate with the fluid. Our analysis therefore predicts that the effect of fluid inertia is to move the particle to the maximum dissipative position (that this is in fact the only maximum will be demonstrated in §4).

In order to obtain a more rigorous result, the entire lift tensor was calculated; the details are given in appendix A. The calculation was quite lengthy and it would have been difficult to justify on the basis of this problem alone. However, the results obtained are applicable to the motion of any three-dimensional body in a linear shear flow. The calculation was therefore justifiable on the basis of the general usefulness of the result.

In order to observe the motion of a dumb-bell shaped particle in a shear flow an experiment was conducted, the results of which are discussed in detail in §5. It is only necessary to mention here that the number of revolutions required for the particle to move into the maximum dissipative orbit was in good agreement with the prediction. The experimental results may be interpreted as confirmation of the predicted stable configuration and the value of the $\mathscr{S}^*$ perturbation.†

4. Dissipation and viscosity

The determination of the intrinsic viscosity of a dilute suspension of dumb-bell shaped particles, in the absence of Brownian motion, may be calculated on the basis of the Stokes approximation, in accordance with the definitions given by Brenner (1958).

† The $\mathscr{S}^*$ component of the lift tensor was found to be a factor of 4π smaller than that originally published by Saffman.

Before making this calculation we will modify (21) and (22) to take into account the effect of interaction between the spheres. We define $\mathbf{U}_B^A$ as the disturbance at sphere A due to the motion of sphere B. The Stokes drag on sphere A is then given by

$$\mathbf{F}^A = 6\pi\mu_0 a\{\mathbf{V}^A - (\boldsymbol{\omega}\times l\mathbf{i}) + \mathbf{U}_B^A\}, \tag{23}$$

where $\boldsymbol{\omega}$ is the angular velocity of the dumb-bell. The velocity field, $\mathbf{U}_B$, resulting from the motion of sphere B may be determined approximately by considering it to be the result of a point force $\mathbf{F}^B$ acting at the centre of sphere B (Happel & Brenner 1965),

$$\mathbf{U}_B = -\frac{\mathbf{F}^B}{6\pi\mu_0 r} - \frac{r^2}{24\pi\mu_0}\nabla[\mathbf{F}^B.\nabla]\frac{\mathbf{1}}{r}, \tag{24}$$

where $\mathbf{F}^B$ is taken to be

$$\mathbf{F}^B = 6\pi\mu_0 a[\mathbf{V}^B - \boldsymbol{\omega}\times(-l)\mathbf{i}] \tag{25}$$

and

$$r^2 = (x-l)^2 + y^2 + z^2. \tag{26}$$

The drag on sphere A is then

$$\frac{\mathbf{F}^A}{6\pi\mu_0 a} = (1+\tfrac{3}{4}\epsilon)(\kappa m_1 n_1 l)\mathbf{i} + (1+\tfrac{3}{8}\epsilon)[\kappa m_1 n_1 l - l\omega_z]\mathbf{j} + (1+\tfrac{3}{8}\epsilon)[\kappa m_1 n_3 l + l\omega_y]\mathbf{k}. \tag{27}$$

As a result of the additional term representing the interaction between the spheres, (21) and (22) are modified in such a way that

$$\alpha(\epsilon) = \tfrac{2}{3}\epsilon^2(1-\tfrac{3}{8}\epsilon). \tag{28}$$

The accuracy of this correction term is demonstrated experimentally in § 5.

Returning to the subject of dissipation, we are interested in the additional dissipation, caused by the presence of sphere A, in a linear shear flow. This is

$$E^* = \epsilon l\mu_0[\mathbf{V}^A - (\boldsymbol{\omega}\times l\mathbf{i}) + \mathbf{U}_B^A]^2 + O(\epsilon^3), \tag{29}$$

which may be rewritten to $O(\epsilon^2)$ as

$$E^* = 6\pi\kappa l^3\mu_0(\epsilon + \tfrac{3}{2}\epsilon^2)\frac{\sin^2\phi\cos^2\phi\sin^4\theta}{[\cos^2\phi + \alpha(\epsilon)]}. \tag{30}$$

A time average dissipation rate, E^*_{av}, for the dumb-bell may be defined as

$$E^*_{\mathrm{av}} = 2\sqrt{6}\,\kappa^2 l^3\mu_0\epsilon^2 F(\theta_0,\epsilon) + O(\epsilon^3), \tag{31}$$

where

$$F(\theta_0,\epsilon) = \int_0^{2\pi} \frac{\sin^2\phi\cos^2\phi\,d\phi}{[\cos^2\phi+\alpha(\epsilon)]\left[1+\dfrac{\cos^2\phi+\alpha(\epsilon)}{\{1+\alpha(\epsilon)\}\tan^2\theta_0}\right]^2},$$

and where we have used (22) for the period as well as the result

$$d\phi/dt^* = \cos^2\phi + \alpha(\epsilon) \tag{32}$$

from the Stokes solution. The dissipation, to the order given in (31), is due to the frictional drag created by a component of cross-flow along the axis connecting the spheres; the cross-flow arises because of the constraint between the spheres.

When the dumb-bell axis coincides with the vorticity vector, $\theta_0 = 0$, the dissipation is $O(\epsilon^3)$, whereas when $\theta_0 = \frac{1}{2}\pi$ the dissipation is a maximum. Also, the dissipation increases monotonically with θ_0 so that there are no local maxima between $\theta_0 = 0$ and $\theta_0 = \frac{1}{2}\pi$.

The viscosity of a dilute suspension of dumb-bell shaped particles is defined as

$$\frac{\mu}{\mu_0} = \sum_A \frac{[\mathbf{V}^A \cdot \mathbf{F}^A + \frac{1}{4}(\nabla \times \mathbf{V})_A \cdot \mathbf{T}^A + \frac{10}{3}\pi a^3 \mu_0 \phi_A]}{\mu_0 \int \Phi \, dQ}, \tag{33}$$

where the subscript denotes the 'centre' of sphere A and the summation is over all spheres. Φ is the Rayleigh dissipation function connected with the undisturbed motion $\mathbf{V}$ and Q is the volume of the suspension; the remaining terms retain their original definition.

The first term in the summation, which accounts for sphere translation relative to the surrounding fluid, includes the effect of interaction between the two spheres of a given dumb-bell, because this effect is of the same order, $O(\epsilon^3)$, as the second and third terms of the summation. All other interaction effects are considered to be of higher order.

When the particles are in the minimum dissipative position, the only non-zero term in the summation is the one involving the dissipation function, since the spheres are moving and rotating with the fluid. In that case, if the particles are uniformly distributed, or if the undisturbed shear flow is linear, the intrinsic viscosity will be Einstein's value of $\frac{5}{2}$. The intrinsic viscosity for other orientations of dumb-bell shaped particles in a linear shear flow may be calculated by evaluating (33); of course the unsteady terms appearing in the equation must be averaged as was done in obtaining (31). The intrinsic viscosity corresponding to the maximum dissipative orbit is of particular interest because of the predicted stability of that configuration. The maximum intrinsic viscosity has been calculated to be

$$\nu_{\max} = \frac{1{\cdot}84}{\epsilon} + 3{\cdot}5 + O(\epsilon). \tag{34}$$

It should be emphasized that this definition of viscosity is based on energy dissipation. A more general discussion of the rheology of solutions of dumb-bells is beyond the scope of this paper.

5. Experiment

In order to obtain general confirmation of the predicted motion, a large cylindrical Couette-flow apparatus was constructed. A 12 in. diameter glass cylinder, 12 in. in length, was placed on a rotating turntable driven by a fractional horsepower motor. A 4 in. diameter cylinder of the same length and closed at the bottom was mounted coaxially within the larger cylinder. A small bearing at the centre of the turntable kept the inner cylinder centred and allowed it to be rotated independently by means of another motor at the top of the apparatus. The bottom 2 in. of the annular region between the two cylinders was filled with distilled water in order to reduce end effects. The remainder of the apparatus was filled with castor oil, the flow field of which was determined to be one-dimensional

by measuring the circular velocity of a very small piece of neutrally buoyant plastic at various radial locations and depths.

Several dumb-bell shaped particles were constructed from $\frac{1}{4}$ in. diameter centreless ground polyethylene and polypropylene spheres, which were slightly buoyant; the specific gravities varied between 0·92 and 0·94 while that of the castor oil was 0·96. Small holes, 0·007 in. in diameter, were drilled on each sphere

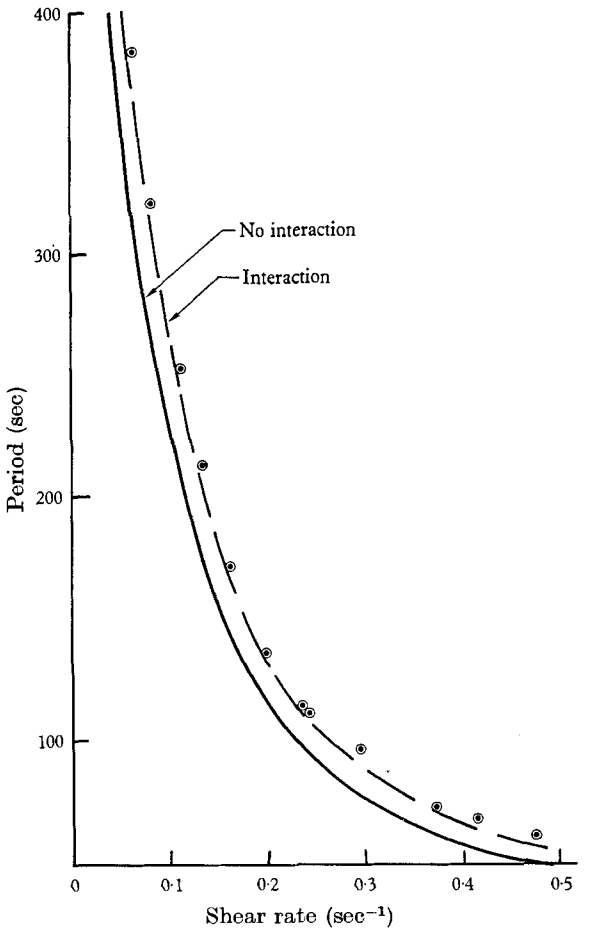

FIGURE 2. Prediction for the period as a function of shear rate. Experimental values, ⊙, for $\epsilon = 0{\cdot}30$.

diameter and the spheres were connected with 0·010–0·012 in. diameter tempered wires. The wire length was adjusted so that the dumb-bells suspended in castor oil. The particles were 'balanced', by making minute adjustments of the amount of wire within each sphere, until the dumb-bells exhibited no preferred orientation when they were suspended in stationary fluid.

The shear rate for a given test was taken to be that at the centre of the dumb-bell. The location of the dumb-bell was determined by aligning a sighting device at the top of the apparatus with a grid scribed on the turntable. The shear rate was varied by placing the centre of the particle at different radial locations and

by employing various combinations of motor speeds. It was also possible to hold the particles fixed for short periods by counter-rotating the cylinders, thus minimizing Coriolis forces.

In order to develop confidence in the experimental apparatus and simultaneously check the first-order solution ($R_\kappa = 0$), the period of rotation of the dumb-bells was measured as a function of the shear rate, κ, and aspect ratio, ϵ. It was possible to measure the period accurately to within a few per cent because the particle swept past the radial lines scribed on the turntable very rapidly

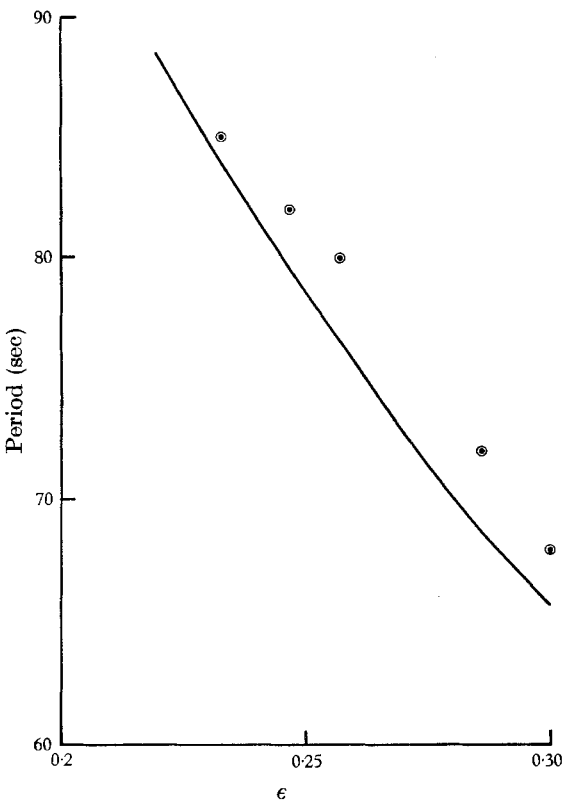

FIGURE 3. Prediction for the period as a function of ϵ. Experimental values, ⊙, for $\kappa = 0{\cdot}411\ \text{sec}^{-1}$.

while spending a much longer time in a tangential direction. This unsteady motion is predicted by the Stokes solution (equation (32)). The first-order solution for the period of rotation is compared with the experimental results in figure 2. The analytical results are presented with and without the effect of interaction between the spheres (equation (28)) for the experimental value of the aspect ratio $\epsilon = 0{\cdot}30$. The effect of aspect ratio on the period, for a given shear rate, is shown in figure 3. The agreement between prediction and experiment appears to improve for decreasing values of ϵ.

The main purpose of the experiment was to ascertain the stability of the maximum dissipative orbit. In order to do this it was necessary to assess second-order

effects, other than fluid inertia, present in the experiment. Since the centres of gravity and buoyancy of the dumb-bell could not be expected to coincide exactly, it must be assumed that some small resultant couple was acting, except when the line connecting the two points was vertical. This effect was minimized by balancing the particle in stationary fluid. However, the natural convection present in the oil presented a limitation on this procedure; it was possible to reduce the rate of rotation below a half a degree per minute in the static fluid. It is felt that in a shear flow this small imbalance was not significant in altering the orbit, except near the (horizontal) maximum dissipative position, because of the averaging effect of the axial component of rotation. Small amounts of curvature in the wire connecting the two spheres also affected the observed equilibrium orientation. For these reasons each test case was composed of two runs employing the same starting angle, θ_0, but with the dumb-bell reversed in direction. In no cases were the particles observed to gravitate toward the (vertical) minimum dissipative position. In most of the cases the particles assumed the same equilibrium orbit from both directions. These final orbits had the appearance of the Stokes solution (21) with values of θ_0 which varied between 85 and 95 degrees, indicating a balance between fluid inertia and the other second-order effects described above. The following table gives values of the experimental parameters which are typical of those used to observe the particle motion:

Sphere material	Polypropylene
Sphere diameter (in.)	0·248
Aspect ratio, ϵ	0·247
Exposed wire length (in.)	0·757
Wire diameter (in.)	0·010
Shear rate ($\sec^{-1}$)	0·415
Period (sec)	82
R_κ	$4{\cdot}1 \times 10^{-3}$

Figure 4 depicts the solution of (20) for the values of ϵ and R_κ given in the table above, and for a value of θ_0 of 45 degrees. Figure 5 compares estimates of the nutation angle, θ, based on visual observation, with predicted values. Both the prediction and the observations are of the minimum nutation angles occurring in a revolution, that is at integer values of ϕ/π. The observations must be regarded as having a tolerance of about five degrees. In order to avoid the problem of starting transients in the fluid the particle was allowed to make a few revolutions before the observations were recorded. The number of revolutions required to reach the equilibrium orbit increased with the diameter and exposed length of the wire connecting the spheres. When the wire diameter exceeded 0·12 in. the rate of gravitation towards a preferred orbit was extremely small. It should also be noted that the requirement, $R_\kappa \ll \epsilon$, imposed in the analysis was not well fulfilled in the experiment. However, it was not feasible to reduce the shear rate drastically because of the rapid increase of the period (figure 2), and the use of more viscous fluids was rejected in order to avoid the possibility of introducing non-Newtonian effects. It is felt that the experiment generally confirmed the

second-order effect of fluid inertia, subject to the stated qualifications regarding other second-order effects present in the experiment.

The authors would like to acknowledge the advice of Professors Philip Saffman and Howard Brenner. The authors are also indebted to an anonymous referee, whose comments led to a great improvement in this paper. This research was supported by the Army Research Office (Durham) under Grant DA-ARO-D-31-124-G649 and by the National Aeronautics and Space Administration.

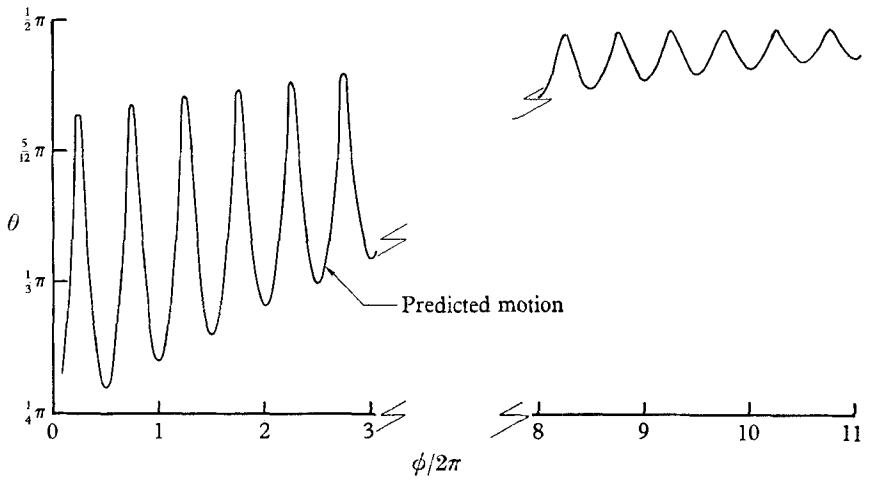

FIGURE 4. Solution of equation (20) for $c = 0{\cdot}25$, $R_\kappa = 4{\cdot}1 \times 10^{-3}$.

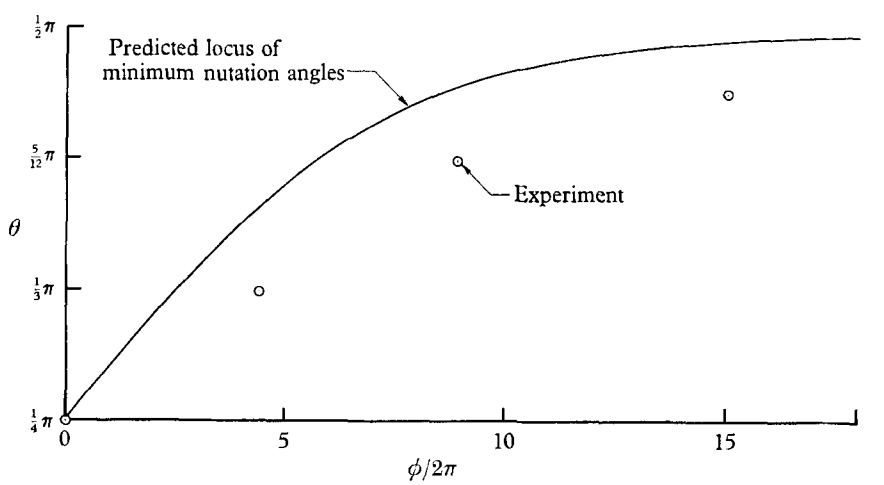

FIGURE 5. Comparison of prediction and experiment for integer values of ϕ/π.

Appendix A

The method used for determining the lift force on a three-dimensional body moving in a linear shear flow is outlined in this appendix. The expression for the lift, which is given to $O(R_\kappa^{\frac{1}{2}})$, is applicable to any three-dimensional body for which the Stokes drag is known, unlike the Oseen correction for uniform flow

(Brenner 1961; Chester 1962) which is restricted to bodies with fore–aft symmetry. We define a lift tensor, L_{jk}, by

$$F_i = \mathscr{D}_{ij}[U_j + (R_\kappa^{\frac{1}{2}} L_{jk} \mathscr{D}_{kl} U_l/\mu a)], \tag{A 1}$$

where **F** is the force on the body and **U** is the relative velocity of the fluid with respect to the body. The Stokes drag, **D***s*, is given by

$$Ds_i = \mathscr{D}_{ij} U_j. \tag{A 2}$$

The lift tensor, which is independent of the shape of the body, is found to be

$$L_{ij} = \begin{pmatrix} 5{\cdot}01 & 0 & 3{\cdot}29 \\ 0 & 3{\cdot}73 & 0 \\ 1{\cdot}82 & 0 & 1{\cdot}73 \end{pmatrix} \times 10^{-2}. \tag{A 3}$$

The calculation of L_{ij} involves a straightforward extension of the original work of Saffman (1965). The co-ordinate system employed in this appendix is therefore in accord with that of Saffman, rather than the system used in the main body of this text.

The exact problem is described by the following equations:

$$\rho \mathbf{u}.\nabla \mathbf{u} = -\nabla P + \mu \nabla^2 \mathbf{u}, \tag{A 4}$$

$$\nabla.\mathbf{u} = 0, \tag{A 5}$$

$$\mathbf{u} = \boldsymbol{\Omega} \times \mathbf{r} \quad \text{on the body}, \tag{A 6}$$

$$\mathbf{u} \to \mathbf{U} + \kappa z \mathbf{i} \quad \text{as} \quad r \to \infty. \tag{A 7}$$

We now introduce the perturbations **q** and p by letting

$$\mathbf{u} = (\mathbf{U} + \kappa x \mathbf{i}) + \mathbf{q}, \tag{A 8}$$

$$P = \kappa U_z x + p, \tag{A 9}$$

where the subscript denotes the z component of **U**. The pressure gradient $\kappa U_z \mathbf{i}$ is required in order that the undisturbed flow be a solution of the Navier–Stokes equations. The problem for the perturbation becomes

$$\rho[(\mathbf{U} + \kappa z \mathbf{i}) + q].\nabla \mathbf{q} + \mathbf{i} \kappa q_z = -\nabla p + \mu \nabla^2 \mathbf{q}, \tag{A 10}$$

$$\nabla.\mathbf{q} = 0, \tag{A 11}$$

$$\mathbf{q} = -\mathbf{U} - \kappa z \mathbf{i} + \boldsymbol{\Omega} \times \mathbf{r} \quad \text{on the body}, \tag{A 12}$$

$$q \to 0 \quad \text{as} \quad r \to \infty. \tag{A 13}$$

An asymptotic solution of these equations may be obtained by the method of matched asymptotic expansions. We note that three Reynolds numbers may be formed corresponding to the characteristic velocities $U = U$, κa and Ωa, where a represents the characteristic body dimension. The parameters appearing in the problem are thus

$$R_v = \rho U a/\mu, \quad R_\kappa = \rho \kappa a^2/\mu, \quad R_\Omega = \rho \Omega a^2/\mu. \tag{A 14}$$

We consider these parameters to play an equally important role as they become very small, i.e.

$$O(R_v) = O(R_\kappa) = O(R_\Omega). \tag{A 15}$$

Our assumption regarding the orders of the Reynolds numbers is more restrictive than, but consistent with, the requirement given by Saffman.

$$R_v \ll R_\kappa^{\frac{1}{2}}, \quad R_\kappa \ll 1, \quad R_\Omega \ll 1. \tag{A 16}$$

Because the three characteristic velocities are of equal order, equation (A 15), the way in which we non-dimensionalize the perturbation velocity is arbitrary. We define

$$\mathbf{q}^* = \mathbf{q}/U. \tag{A 17}$$

The differential equations which appropriately describe $\mathbf{q}^*$ to a given order depend on which region of the flow field is under consideration. We therefore introduce a length scale l, defined by

$$l/a = 1/R_\kappa^\sigma, \quad (0 \leqslant \sigma), \tag{A 18}$$

and an intermediate variable, x_i^*, by

$$x_i^* = x_i/l. \tag{A 19}$$

x_i^* corresponds to the Stokes variable when $\sigma = 0$; when $\sigma = \frac{1}{2}$, x_i^* becomes the outer variable used by Saffman (1965). We obtain the following equation of momentum in x_i^* variables:

$$R_\kappa^{1-\sigma}\alpha(\mathbf{U}^* + \mathbf{q}^*).\nabla^*\mathbf{q}^* + R_\kappa^{1-2\sigma}\left[z^*\frac{\partial \mathbf{q}^*}{\partial x^*} + \mathbf{i}q_z^*\right] = -\nabla p^* + \nabla^{*2}\mathbf{q}^* + R_\kappa^\sigma \mathbf{D}s^*\delta(r^*) \tag{A 20}$$

where $\alpha = R_v/R_\kappa = O(1)$, $U^* = U/|U|$ and $p^* = pl/\mu U$. The dimensionless pressure perturbation, p^*, has the same magnitude as the viscous stress throughout the flow field. The last term on the right-hand side represents a concentrated force acting at the origin; $\mathbf{D}s^*$ is the dimensionless Stokes drag, $\mathbf{D}s^* = \mathbf{D}s/\mu U a$. For values of $x_i \gg a$, corresponding to $\sigma > 0$, the forcing term replaces the boundary condition on the surface of the body. The resulting solution describes the first-order velocity perturbation at distances exceeding the body dimension (Chang 1960; Chang & Finn 1961; Childress 1964). For values of $x_i = O(a)$, corresponding to $\sigma = 0$, the exact boundary condition (A 12) must be used.

In order to study the magnitude of q^* and the appropriate governing equations, it is convenient to think of the flow field as being divided into two regimes: (i) $0 \leqslant \sigma < \frac{1}{2}$ and (iii) $\frac{1}{2} < \sigma$, separated by a region, (ii) $\sigma = \frac{1}{2}$, we will call the Saffman region. We observe from (A 20) that, for $\sigma > \frac{1}{2}$, the forcing term, which represents the effect of the body, is of order $o(R_\kappa^{\frac{1}{2}})$. This, together with the boundary condition $q^* \to 0$ as $r^* \to \infty$, implies that $q^* = o(R_\kappa^{\frac{1}{2}})$ in regime (iii). When $\sigma = \frac{1}{2}$, the requirement that the transport and forcing terms be of the same order indicates that the perturbation q^* is $O(R_\kappa^{\frac{1}{2}})$. Equation (A 20) reduces, in the limit $R_\kappa \to 0$, to

$$\left[z^*\frac{\partial \mathbf{q}^*}{\partial x^*} + \mathbf{i}q_z^*\right] = -\nabla^* p^* + \nabla^{*2} q^* + R_\kappa^{\frac{1}{2}}\mathbf{D}^*\delta(r^*), \tag{A 21}$$

which is the dimensionless form of Saffman's (1965) equation (3.10). When $0 \leqslant \sigma < \frac{1}{2}$, and $O(R_\kappa^{\frac{1}{2}}) < q^* \leqslant O(1)$, the transport term in (A 20) is of higher order than the viscous term. Between the body and the Saffman region the flow is

approximated *uniformly* to $O(R_\kappa^{\frac{1}{2}})$ by a *Stokes solution* (Kaplun 1967). We conclude, therefore, that the Saffman equation, (A 21), with the delta function replaced by the exact boundary conditions (A 12) and (A 13), yields a uniformly valid solution for the entire flow field to $O(R_\kappa^{\frac{1}{2}})$. In terms of the method of inner and outer expansions, (A 21) is the outer equation. The inner equation, to $O(R_\kappa^{\frac{1}{2}})$, is the Stokes equation and the body shape is characterized by the Stokes drag. The matching procedure is valid for any three-dimensional body for which the Stokes drag is known. In addition, the rotation of the body and the linear shear of the undisturbed field do not give rise to drag, as is demonstrated by Faxen's law.

We proceed to find the lift tensor by considering the fundamental solution of (A 21) for a unit force, **d**, in the direction of the Stokes drag **D***s*. The corresponding velocity and pressure perturbations, q' and p', are defined by the relations

$$\mathbf{q}^* = R_\kappa^{\frac{1}{2}}|\mathbf{D}s^*|\,\mathbf{q}', \quad p^* = R_\kappa^{\frac{1}{2}}|Ds^*|\,p'. \tag{A 22}$$

We solve the resulting equation

$$\nabla^* p' - \nabla^{*2}\mathbf{q}' + \left[z^* \frac{\partial \mathbf{q}'}{\partial x^*} + \mathbf{i}q_z'\right] = \mathbf{d}^*\,\delta(r^*) \tag{A 23}$$

by introducing the Fourier transform

$$\mathbf{\Gamma} = \frac{1}{8\pi^3}\int_{-\infty}^{\infty} \mathbf{q}'\, e^{ik.r^*}\, d\mathbf{r}^*, \quad \mathbf{q} = \int_{-\infty}^{\infty} \mathbf{\Gamma}\, e^{-ik.r^*}\, d\mathbf{k}. \tag{A 24}$$

The components of $\mathbf{\Gamma}$ are

$$\begin{aligned}
-k_1\frac{\partial \Gamma_1}{\partial k_3} + \Gamma_3 - 2\frac{k_1^2}{k^2}\Gamma_3 + k^2\Gamma_1 &= \frac{k_1}{k^2}\Sigma A_j k_j - A_1,\\
-k_1\frac{\partial \Gamma_2}{\partial k_3} - 2\frac{k_1 k_2}{k^2}\Gamma_3 + k^2\Gamma_2 &= \frac{k_2}{k^2}\Sigma A_j k_j - A_2,\\
-k_1\frac{\partial \Gamma_3}{\partial k_3} - 2\frac{k_1 k_3}{k^2}\Gamma_3 + k^2\Gamma_3 &= \frac{k_3}{k^2}\Sigma A_j k_j - A_3,\\
k_1\Gamma_1 + k_2\Gamma_2 + k_3\Gamma_3 &= 0,
\end{aligned} \tag{A 25}$$

where $k^2 = k_1^2 + k_2^2 + k_3^2$,

and $A_j = d_j/8\pi^3$. (A 26)

We now define q'_{ij}, and the corresponding transform, Γ_{ij}, by

$$q_1 = \sum_{j=1}^{3} q_{ij}, \quad \Gamma_1 = \sum_{j=1}^{3} \Gamma_{ij}, \tag{A 27}$$

where q_{ij} is the velocity perturbation along the i-axis due to the component of $\mathbf{d}^*$ along the j-axis. The Fourier transforms of these velocity perturbations are then given by

$$\Gamma_{11} = -\int_0^\infty \{F_{11}(k_1, k_2, k_1\xi + k_3)\, e^{-\beta}\}\, d\xi,$$

where

$$F_{11} = A_1\left(1 - \frac{k_1^2}{k^2}\right) + \Gamma_{31}\left(1 - \frac{2k_1^2}{k^2}\right);$$

$$\Gamma_{13} = -\int_0^\infty \{F_{13}(k_1, k_2, k_1\xi + k_3)\, e^{-\beta}\}\, d\xi,$$

where
$$F_{13} = A_3 \frac{k_3}{k^2} + \Gamma_{33}\left(1 - \frac{2k_1}{k^2}\right);$$

$$\Gamma_{22} = -\int_0^\infty \{F_{22}(k_1, k_2, k_1\xi + k_3)\, e^{-\beta}\} d\xi, \tag{A 28}$$

where
$$F_{22} = A_2\left(\frac{k_1^2 + k_3^2}{k^2}\right) - \Gamma_{32}\left(\frac{2k_1 k_2}{k^2}\right);$$

$$\Gamma_{31} = \int_0^\infty \left\{A_1\left(\frac{k_1^2\xi + k_1 k_3}{k^2}\right) e^{-\beta}\right\} d\xi,$$

$$\Gamma_{32} = \int_0^\infty \left\{A_2\left(\frac{k_1 k_2 \xi + k_2 k_3}{k^2}\right) e^{-\beta}\right\} d\xi,$$

$$\Gamma_{33} = -\int_0^\infty \left\{A_3\left(\frac{k_1^2 + k_2^2}{k^2}\right) e^{-\beta}\right\} d\xi,$$

and where
$$\beta = \xi\left(k^2 + k_1 k_3 \xi + \frac{k_1^2 \xi^2}{3}\right). \tag{A 29}$$

The perturbations q'_{12}, q'_{21}, q'_{23} and q'_{32} are zero because of the symmetry of the linear shear flow; e.g. Γ_{32} is odd in k_2. It should be noted that Γ_{32} is not zero but is symmetric and this symmetry is lost when it is multiplied by k_2 in the term F_{22}.

The components of the lift tensor, L_{ij}, are given by

$$L_{ij} = \bar{q}_{ij}/d_j^* \quad \text{(no summation)}, \tag{A 30}$$

where the $\bar{q}_{ij}$ represent the regular parts of the velocity perturbations, q'_{ij}, at the origin, that is, at the body. If we denote the Stokeslets by qs'_{ij}, then the finite parts may be written as

$$\bar{q}_{ij} = q'_{ij} - qs'_{ij} = \int_{-\infty}^{\infty} (\Gamma_{ij} - \Gamma s_{ij})\, d\mathbf{k}, \tag{A 31}$$

where the Γs_{ij} represent the Fourier transforms of the Stokeslets

$$\left.\begin{aligned} \Gamma s_{11} = \frac{A_1}{k^2}\frac{k_1^2}{k^2} - 1, \quad \Gamma s_{13} = A_3 \frac{k_1 k_3}{k^4}, \quad \Gamma s_{22} = -A_2\left[\frac{k_1^2 + k_3^2}{k^4}\right], \\ \Gamma s_{31} = A_1 \frac{k_1 k_3}{k^4}, \quad \Gamma s_{33} = A_3 \frac{1}{k^2}\left[\frac{k_3^2}{k^2} - 1\right]. \end{aligned}\right\} \tag{A 32}$$

The cancellation of the Stokeslets may be achieved by integrating by parts the portion of each Γ_{ij} containing the singularity. For example, if we consider q'_{31} we may write

$$A_1 \int_0^\infty \left\{\frac{k_1 k_3}{k^2} e^{-\beta}\right\} d\xi = \Gamma s_{31} - A_1 \int_0^\infty \left\{\frac{2\xi k_1^2 k_3^2 + \xi^2 k_1^3 k_3}{k^4} e^{-\beta}\right\} d\xi \tag{A 33}$$

so that $\bar{q}_{31}$ becomes

$$\bar{q}_{31} = A_1 \int_0^\infty d\mathbf{k} \int_0^\infty \left\{\frac{\xi[k_1^2 k^2 - k_1 k_3(2k_1 k_3 + \xi k_1^2)]}{k^4} e^{-\beta}\right\} d\xi.$$

The value of this constant was found to be in agreement with the corrected value given by Saffman (1968, corrigendum).

The constants L_{31} and L_{33} were reduced to double definite integrals, while the remaining components of the lift tensor involved both double and triple integrals. These integrals were evaluated numerically to three-place accuracy.

REFERENCES

BRENNER, H. 1958 *Phys. Fluids*, **1**, 338.

BRENNER, H. 1961 *J. Fluid Mech.* **11**, 604.

CHANG, I-DEE 1960 *J. Fluid Mech.* **9**, 473.

CHANG, I-DEE & FINN, R. 1961 *Arch. Ratl Mech. Anal.* **7**, 388.

CHESTER, W. 1962 *J. Fluid Mech.* **13**, 557.

CHILDRESS, W. S. 1964 *J. Fluid Mech.* **20**, 305.

CHRISTOPHERSON, D. G. & DOWSON, D. 1959 *Proc. Roy. Soc.* A **251**, 550.

COX, R. G. 1965 *J. Fluid Mech.* **23**, 273.

EINSTEIN, A. 1905 *Investigations on the Theory of the Brownian Movement.* New York: Dover.

HAPPEL, J. & BRENNER, H. 1965 *Low Reynolds Number Hydrodynamics*, p. 83. New York: Prentice-Hall.

JEFFERY, G. B. 1922 *Proc. Roy. Soc.* A **102**, 161.

KAPLUN, S. 1967 *Fluid Mechanics and Singular Perturbations*, p. 47. Academic Press.

MASON, S. G., KARNES, A. & GOLDSMITH, H. L. 1963 *Nature, Lond.* **200**, 159.

SAFFMAN, P. G. 1956 *J. Fluid Mech.* **1**, 540.

SAFFMAN, P. G. 1965 *J. Fluid Mech.* **22**, 385.

SAFFMAN, P. G. 1968 *J. Fluid Mech.* **31**, 624.

TAYLOR, G. I. 1923 *Proc. Roy. Soc.* A **102**, 58.